Nuclear Instruments and Methods in Physics Research B xxx (2012) xxx–xxx

Contents lists available at SciVerse ScienceDirect

Nuclear Instruments and Methods in Physics Research B

journal homepage: www.elsevier.com/locate/nimb

Stable platinum isotope measurements in presolar nanodiamonds by TEAMS

A. Wallner [a,b,c,*], K. Melber [a], S. Merchel [d], U. Ott [e], O. Forstner [a], R. Golser [a], W. Kutschera [a], A. Priller [a], P. Steier [a]

[a] University of Vienna, Faculty of Physics, VERA Laboratory, Währinger Strasse 17, A-1090 Vienna, Austria
[b] Department of Nuclear Physics, Research School of Physics and Engineering, The Australian National University, Canberra, Australia
[c] Australian Nuclear Science and Technology Organisation (ANSTO), Lucas Heights, Australia
[d] Helmholtz-Zentrum Dresden-Rossendorf (HZDR), D-01314 Dresden, Germany
[e] Max-Planck-Institut für Chemie, Joh.-J.-Becherweg 27, D-55128 Mainz, Germany

ARTICLE INFO

Article history:
Received 21 July 2011
Received in revised form 17 March 2012
19 March 2012
Available online xxxx

Keywords:
TEAMS
Trace elements
Pt
Super novae
Presolar grains
Nanodiamonds

ABSTRACT

Nanodiamonds are stardust grains commonly found in primitive meteorites. They survived the formation of the solar system and kept their own individuality. Measurements of trace-element isotopic signatures in these grains will help understanding heavy element nucleosynthesis in massive stars and dust formation from their ejecta. We have continued previous attempts to search for stable Pt isotope anomalies in nanodiamonds via trace element accelerator mass spectrometry (TEAMS). The installation of a new injector beam line at the VERA facility allowed studying low traces of stable elements in different materials. Moreover, recent experiments showed that VERA provides the required measurement precision together with a low Pt machine background. Here, we observed for the first time an indication for enhancements of $^{198}Pt/^{195}Pt$ isotope ratios in two diamond residues prepared by different chemical separation techniques from the Allende meteorite. Variations in other isotopic ratios were within analytical uncertainty, and no anomaly was identified in a third diamond fraction.

1. Introduction

Most of the material in meteorites, like terrestrial matter, shows isotopic ratios that are close to the solar system values. Nevertheless in primitive meteorites variations have been preserved that show up as deviations from normal. Such isotope anomalies range from 10^{-4} (sometimes even between bulk meteorites) up to several orders of magnitude. The latter large anomalies are found in grains of stardust that by now have been identified in many primitive meteorites of various types. Often also called presolar grains, they originate as dust formed in the winds of low-mass stars or in the ejecta of supernova events [1]. When the solar system formed, some of these grains were embedded into larger bodies but survived and were not homogenized. Eventually, due to impacts on the meteorite parent bodies, fragments were captured by the Earth and are found as meteorites. Prominent examples of such meteorites in the context of our study are the Murchison and Allende meteorites. Both fell in 1969, in Australia and Mexico, respectively.

As stardust grains found in meteorites kept their own individuality and carry isotopic information that survived the formation of the solar system, they show the imprint of the nucleosynthesis processes taking place in their parent stars. The most abundant grains of stardust chemically isolated from meteorites are nanodiamonds; e.g. they account for 6% of the total carbon content of the Murchison meteorite. Unfortunately, existing laboratory measurements of their isotopic patterns do not allow for a consistent understanding of their origin. The reasons are mainly due to their small size (nm), low abundance of trace elements trapped in these tiny diamonds [2] and the elaborate chemistry required for laboratory measurements. In any case, they were most likely formed in (or affected by) a supernova environment [1]. Measurements of trace-element isotopic signatures will thus help the understanding of heavy element nucleosynthesis in massive stars and dust formation from their ejecta. In particular, the results will allow testing predictions of r-process nucleosynthesis and understanding the uniformity of the "main r-process" [3].

Isotopes of major elements in stardust grains can be analyzed by secondary ion mass spectrometry (SIMS), even in single grains using Nano-SIMS down to few hundred nanometer size, e.g. silicon carbide or corundum (but not nanodiamonds). The situation is different for rare trace elements, however. TIMS and ICP-MS (on assemblages of grains), on the other hand, suffer from the problem of isobaric and molecular interferences that cannot be resolved for most isotopes (see e.g. the overview analysis of s-process rare

* Corresponding author at: University of Vienna, Faculty of Physics, VERA Laboratory, Währinger Strasse 17, A-1090 Vienna, Austria.
E-mail addresses: anton.wallner@univie.ac.at, anton.wallner@anu.edu.au (A. Wallner).

0168-583X/$ - see front matter © 2012 Elsevier B.V. All rights reserved.
http://dx.doi.org/10.1016/j.nimb.2012.03.036

earth elements in silicon carbide grains [4], where only a limited dataset was obtained due to these interferences).

The advantage of accelerator mass spectrometry (AMS) is that it does not suffer from molecular isobaric interferences at all, due to the use of tandem accelerators (and can potentially separate true isobars). Another advantage is its flexibility for switching to different isotopes and elements because scaling is a function of the mass directly. AMS usually deals with isotope ratios (radionuclide to stable isotope) of the order of 10^{-12}–10^{-15}. For applications in trace element analysis, their concentrations are between 10^{-5} and 10^{-9}. Moreover, their difference in isotopic abundances (ratios of stable isotopes) is only a few orders of magnitudes at most. An alternative method to AMS is RIMS (resonance ionization mass spectrometry), which has been used, e.g. to study Zr [5] or Tc [6] isotopes in presolar silicon carbide grains. Although RIMS may also be applicable to Pt isotopes, the greater flexibility of AMS and the prolific production of negative Pt ions make AMS particularly well suited for a Pt isotope study. For a review on different techniques see e.g. [7].

Stable isotope measurements using AMS (trace element AMS, TEAMS) for different applications have been performed previously, e.g. at IsoTrace, Toronto [8,9], Australis [10] and ETH Zurich (with a dedicated ion source for stable isotope measurements) [11,12] and ANSTO. First AMS measurements of Pt isotope ratios in presolar nanodiamonds were performed at TU Munich [13]. They obtained an upper limit for isotope anomalies for two meteorites, Allende and Murchison. However, for quantitative conclusions an improvement in accuracy was required. We continued these measurements at the University of Vienna at the VERA facility, a dedicated AMS facility which should provide the required measurement precision for such applications. These investigations were part of a measurement programme at VERA applying AMS to open questions in nuclear astrophysics [14].

An important issue for studying isotopic effects in nanodiamonds is the necessity of analyzing impurity-free samples i.e. nanodiamonds with bulk meteorite material and traces of other meteorite material, like silicon carbide, removed. The bulk material would dilute the true presolar isotope signature by solar values and the other contaminants might alter this signature with isotope signatures dominated by contributions from other nucleosynthesis events such as s-process isotopes produced in low-mass stars.

2. Nanodiamonds and reference samples for AMS

The grains of interest for our studies are nanodiamonds (average size 2.6 nm). A presolar origin is indicated by previous measurements of the isotopic composition of the trace elements xenon and tellurium [15,16] applying noble gas mass spectrometry and TIMS, respectively. Nanodiamonds consist on average of only 1000 carbon atoms (therefore single grain analysis is not feasible even for carbon), but they are available in large quantities. For an abundance of 10 μg/g Pt in nanodiamonds, a milligram of diamond will contain about 3×10^{13} atoms of Pt. Assuming an overall efficiency for Pt-AMS of 0.1%, a milligram of diamonds will in principle allow the detection of $\approx 3 \times 10^{10}$ Pt atoms. For the chemical isolation of a milligram of diamond ≈3 g of material from the Allende meteorite or 4 g of Murchison meteorite will be sufficient, so ample material is available [13].

Previous ICP-MS analyses of mixed diamond/silicon carbide samples [4] showed that in the mixture diamond and silicon carbide (SiC), the observed signatures were dominated by the s-process pattern of the SiC mainstream grains. Sample material free from SiC can be achieved by choosing as starting material for the extraction a meteorite that is known to contain no SiC, as is the case for the meteorite Allende. In addition, isolation of diamond stardust by microwave chemistry is known to destroy SiC, but leaving diamond intact [13]. This technique was used for further cleaning of some of our nanodiamond samples.

For this work we have used three nanodiamond residues of the same material as analyzed in the previous study at TU Munich [13]. However, only a limited amount of nanodiamonds from the Allende meteorite remained for these first tests at VERA. Additional AMS samples, serving as reference material, were Pt of terrestrial origin, co-precipitated with aluminum hydroxide, transformed into an Al_2O_3 matrix and containing homogenously distributed Pt. Here, sufficient material was available. Both Pt with natural isotopic abundance ("^{nat}Pt" and also highly enriched in ^{198}Pt ("^{198}Pt") were produced at concentrations of 0.1–0.4 μg/g in several mg of Al_2O_3 bulk material [13]. Finally, a mixture of "^{nat}Pt" and "^{198}Pt" was available as well ("^{mix}Pt"). A few mg of material was split into several sputter cathodes. Enriched ^{198}Pt samples were used as monitors for studying ^{nat}Pt background. Background Pt most likely will consist of natural isotope ratios and sensitively lowers the nominal ^{198}Pt/^{195}Pt ratio of these enriched samples. In addition, blank material from pure Cu, Al and Ag powder was produced.

The nanodiamonds were chemically extracted from Allende by the procedures described in detail in [13]: different procedures were tested to optimize processing speed and chemical yield and more important, to purify the nanodiamond fraction by removing most of the other components from the meteorite bulk material. Indications on how much of the non-diamond compounds survived this aggressive treatments are given by neutron activation analysis [13].

For our measurements Allende material from the following different chemical separation procedures was available: AKL, AMW and ACL. AKL was extracted by applying a classical isolation technique [17], AMW had undergone micro wave treatment [13], and ACL originally was AKL material with an additional $HCl/NaClO_3$ treatment with the goal to reduce further some "solar contamination", represented by high concentrations of Ir. Subsequent INAA analysis of these latter samples support such a cleaning effect, solar Ir, Os and Re were reduced only about 10–13%, Pt by about a factor of 2. However, ACL showed higher concentrations of e.g. Mo or W indicating some contamination of unknown origin.

3. AMS measurements of Pt

VERA, based on a 3-MV tandem, is designed to allow AMS measurements up to the heaviest nuclides [18,19]. Its injection system provides high-mass resolution. The high-energy side is equipped with Wienfilter, analyzing magnet, high-resolving 90° electrostatic deflector and a switching magnet. For isotopic suppression a time-of-flight detection system with 2.8 m flight path in combination with an energy-sensitive ionization chamber is used. Such a setup allows efficiently suppressing neighboring masses, e.g. background from ^{235}U and ^{238}U ions mimicking true events in ^{236}U and allows measurements of ^{236}U/^{238}U ratios $\approx 10^{-12}$ [19].

Pt isotope ratio measurements, however, do not require such high isotopic suppression of neighboring isotopes for stable isotope measurements. Pt has six stable isotopes: ^{190,192,194,195,196,198}Pt [20]. The isotopic ratios of these stable Pt isotopes relative to the most abundant ^{195}Pt are between 4×10^{-4} and 0.97. The most interesting isotopes for our work from the nuclear astrophysics point of view are the more abundant $^{194-198}$Pt isotopes: nanodiamonds most likely contain information on r-process nucleosynthesis, which builds up these neutron-rich isotopes, in particular the most neutron-rich ^{198}Pt. The solar abundance ratios for ^{198}Pt/^{195}Pt, ^{196}Pt/^{195}Pt and ^{194}Pt/^{195}Pt are 0.21, 0.75 and 0.97, respectively. A moderate suppression of neighboring isotopes in AMS is sufficient, i.e. time-of-flight, switching magnet and electrostatic deflector are

Please cite this article in press as: A. Wallner et al., Stable platinum isotope measurements in presolar nanodiamonds by TEAMS, Nucl. Instr. Meth. B (2012), http://dx.doi.org/10.1016/j.nimb.2012.03.036

not necessary for such measurements. Possible ambiguities from E/q interference, however, cannot be excluded a priori and an energy measurement of the particles is desirable.

Fortunately, Pt measurements of all the interesting isotopes, ^{194,195,196}Pt and ^{198}Pt, do not suffer from isobaric interferences. For A = 194 and 195 no other stable isotope exists at all. For ^{196,198}Pt stable isobars exist in Hg. However, Hg does not form stable negative ions (for ^{190,192}Pt some interference via Os will exist). Finally, Pt itself does form readily negative ions and high detector count rates can be expected: In nanodiamonds extracted from meteorites Pt may exist at concentrations of 0.1–10 μg/g; i.e. with abundance ratios of 10^{-7}–10^{-5} relative to the bulk material. Nanodiamonds of course consist dominantly of carbon. Usually, we had to run the ion source at low output. For these kinds of measurements no currents were measured, but count rates for the various Pt isotopes in slow-switching mode (several seconds counting time per measurement). Different particle detectors were utilized for systematic studies (see below).

Our first attempts to measure Pt in nanodiamonds were performed with the original MC SNICS ion source (S1) [21]. However, we found high particle count rates of Pt independent of all different kind of samples (>100 cts s^{-1}). This was the case for blank material made from pure Cu, Al and Ag, but also for ^{nat}Pt reference samples. The highly enriched ^{198}Pt reference samples gave isotope ratios close to natural Pt ratios; i.e. indicating a high background count rate of natural Pt signature originating from other sources. We identified two likely sources: (1) memory of previous macroscopic Pt beams; and (2) intrinsic contamination with Pt in the Ag powder which was used as a binder in the sputter cathodes.

At VERA intense macroscopic Pt beams were produced in previous years mainly for studying the beam optics at the injection side of the facility. Most likely, such Pt still exists in the ion source and becomes repeatedly ionized again. Remarkably, such high memory effects were not observed at the single cathode ion source at TU Munich [13]. The high Pt count rates originating from source S1 did not allow the investigation of trace levels of Pt in nanodiamonds. Interestingly, the first AMS measurements at TU Munich on Pt in nanodiamonds were performed on sputter samples with the nanodiamonds mixed into Ag powder [13]. This Ag powder was shown to be itself low in Pt concentration. Platinum count rates of ≈0.1–1 cts s^{-1} were observed for Ag blank material. At VERA we used the same Ag material (Alfa Aesar), however, from a different lot, for which we found high Pt count rates. Typical values were 10^2–10^3 counts per second, approx. 2–3 orders of magnitude higher than other "clean" Cu or Al blanks, and even 10–50 times higher than our 0.1–0.4 μg/g reference samples. This effect was somewhat hidden because of the intrinsic Pt count rate originating from the ion source itself.

The extension of VERA with a second identical MC-SNICS ion source (S2) [22] allowed us focusing on TEAMS measurements again.

Platinum readily forms negative ions (electron affinity of 2.13 eV). We used monoisotopic ^{197}Au for tuning the machine. Since Au also readily forms negative ions, the ion source was usually operated at moderate settings, i.e. at low ionizer power and limited Cs supply. A negative ion current of a few hundred nA $^{197}Au^-$ was injected into the tandem accelerator. The terminal voltage was set between 2.8 and 3 MV. We selected the 4^+ charge state (charge state yield of ≈6% for Au and Pt). After passing the analyzing magnet, the beam was filtered with a 90° electrostatic deflector before entering a particle detector. At VERA the suppression of neighboring isotopes in this mass range is sufficiently high; no interference from ^{197}Au was detected when scaled to A = 198 after tuning.

Tuning at VERA usually makes use of the automax program [23]. The final setup for A = 197 was performed with an attenuated beam directed into the particle detector. The setup for the various Pt isotopes, i.e. for A = 194, 195, 196 and 198 was then scaled from the ^{197}Au setup. We realized that a small improvement in transmission was achieved by individually tuning the various masses for the most critical parameters in a last step, mainly the mass-sensitive bouncer voltage at the low energy side, and some horizontal and vertical steerers. This individual tuning step also led to closer agreement of the measured Pt ratios with respect to their natural values.

The typical measurement procedure for Pt measurements was the following: a sample wheel with 40 positions was loaded with several tuning, blank, reference and with the nanodiamond samples. Due to the much higher concentrations of Pt in the nanodiamond samples, some cross talk to blank samples was observed. However, this cross talk was of the order of 10^{-4} and no significant corrections in the measured ratios were required. The blank, reference and nanodiamond samples were measured in a batch mode with approx. 30–45 min measuring time per run and 3–7 runs per sample.

We normalized all our Pt count rates to ^{195}Pt. Therefore, all other isotopes were sandwiched between ^{195}Pt measurements. A typical sequence of count rate measurements was 195-198-195-196-195-194-195. Such a sequence was repeated 3–6 times and defined one run on an individual sample. The measuring time for one mass was typically 10 s. It has to be noted that the switching time between the masses was of similar duration as the measurement period. In the last measurement series, the switching time was reduced to about 4 s.

The Pt count rates were between a few detector events per second for fresh blanks and up to several thousand for the highest nanodiamond sample. We found that the first ratios of a run resulted consistently in somewhat lower values – indicating a non-linear increase in the count rates for the first minutes of sputtering. Usually these first data were not used for calculating mean values.

Counting statistics was never the most important contributor to the overall uncertainty, which was rather dominated by the non-linear change in the Pt count rates during the time when switching from one mass to the next. Such effects resulted in some random scatter of the isotope ratios within a run. We observed a slightly different transmission of the four Pt isotopes resulting in small deviations of measured to nominal ratios in the reference samples. These differences to the nominal values were up to 8% (see Section 4). The deviations were assumed to be the same for unknown and known samples and a scaling factor was applied to adjust for these differences. Its uncertainty (typically of the order of 1–2%.) was calculated from the standard deviation of the mean value of the reference material.

Using source S2 [22], we still observed enhanced ^{195}Pt events when measuring ^{198}Pt-enriched samples. Used "^{198}Pt" samples started with ^{198}Pt/^{195}Pt ratios well below their expected ratios indicating surface contamination with ^{nat}Pt or memory in the ion source (some nanodiamonds had orders of magnitude higher count rates). During the measurement the "^{198}Pt" samples showed steadily increasing ^{198}Pt/^{195}Pt ratios indicating a cleaning effect during sputtering. However, these unknown sources of ^{nat}Pt did not affect the results for the unknown samples (nanodiamonds), as their count rates (i.e. Pt concentrations in the nanodiamonds) usually were the highest ones and only small corrections, if at all, were required (see below). Some A/q ambiguities were observed, in particular for A = 196 ($^{196}Pt^{4+}$), which exactly fits for A = 49, 98 and 147 in charge states 1^+, 2^+ and 3^+, respectively, and therefore enter the final detector system. However, the energy of these background ions is different and the count rates were low, so no pile-up interfered with the Pt^{4+} signals. Simultaneous detection of the molecular breakup products in the particle detector would result in the same

Please cite this article in press as: A. Wallner et al., Stable platinum isotope measurements in presolar nanodiamonds by TEAMS, Nucl. Instr. Meth. B (2012), http://dx.doi.org/10.1016/j.nimb.2012.03.036

energy deposited and hence would mimic a true Pt signal. However, in these cases a significantly higher count rate originating from the single background particles with their lower energies should be visible in the energy spectra as well (it is much more likely that a charge state combination in the stripper is generated for the break-up products which does not fit simultaneously both conditions required for them to pass all filters). We have not found any indication in our energy spectra that molecular break-up products could contribute to erroneous background counts. Moreover, the Pt^{4+} ions were dominating the count rate in the particle detector for reference and nanodiamond samples.

As can be seen in Table 1, the ^{195}Pt detector count rate for the blanks (col. 3) was usually low and increased from about 0.5 cts s^{-1} to about 10–30 cts s^{-1} during the various measurement series. This increase is mainly interpreted being due to a general higher source output for the later measurements. Still, because of the nearly exhausted nanodiamond material of AKL and in particular AMW, some small Pt background corrections had to be applied in these cases: the difference in the ratio $^{198}Pt/^{195}Pt$ for nanodiamond samples to the ^{nat}Pt samples was 10% at most (see Section 4). So, a rough estimate for the blank contribution in the most extreme case (highest background for the lowest nanodiamond sample AMW in measurement 07) results in a 20% contribution from external Pt to the total ^{198}Pt count rate. This would lower the measured isotope ratio $^{198}Pt/^{195}Pt$ by 20% × 10%, i.e. would cause a relative downshift of 2% in the isotope ratio $^{198}Pt/^{195}Pt$. However, usually the background corrections were much smaller and they did not affect the final uncertainty.

4. AMS results for nanodiamonds extracted from Allende

Table 2 lists the mean isotope ratios as measured in four beamtimes (“Pt_05” to “Pt_08”) and not normalized to any reference material. ^{nat}Pt denotes Pt of natural composition mixed into Al_2O_3 matrix (reference samples, ca. 0.4 μg/g). The uncertainties given represent the standard deviation of the mean and are in most cases <1%. Comparing results from different measurement series, shows that additional uncertainty contributions dominate the final values (see below). Table 3 lists all data for the nanodiamond samples obtained from the four measurement series (col. “Pt_05” to “Pt_08” as values relative to the reference sample. Column six (“mean”) shows the unweighted mean of all four measurements. The natural isotope ratios (relative to ^{195}Pt) are listed in the first line of the corresponding 3 sections: 0.212, 0.746 and 0.974 for $^{198}Pt/^{195}Pt$, $^{196}Pt/^{195}Pt$, and $^{194}Pt/^{195}Pt$, respectively. For ^{nat}Pt, their measured ratios (uncorrected, e.g. ^{nat}Pt-198 for $^{198}Pt/^{195}Pt|_{meas}$) and the relative deviation of the measured ratio from the nominal Pt isotope ratio, (“rel. dev. to $^{198}Pt/^{195}Pt|_{nat}$”); i.e. $[(^{198}Pt/^{195}Pt)|_{meas}-(^{198}Pt/^{195}Pt)|_{nat}]/[^{198}Pt/^{195}Pt)|_{nat}]$ are listed in the two following lines. Below that, the measured Pt isotope ratios for the three different nanodiamond fractions available from the Allende meteorite are listed (e.g. “ACL-198”) as ratios relative to the measured ^{nat}Pt-values, (i.e. $(^{198}Pt/^{195}Pt|_{ACL})/(^{198}Pt/^{195}Pt|_{natPt})$, and similar ratios for ^{196}Pt and ^{194}Pt) are given. For the reference samples the deviations of measured isotope ratios to the nominal values are given in %-deviations to underline the scaling required for normalizing the measured ratios, which was between −7% and +5%. The results for the meteorite samples, however, are given as data relative to the reference materials, i.e. the measured ratios of meteorite samples divided by the measured ratios of the reference sample $[(^{198}Pt/^{195}Pt)|_{meteorite}/(^{198}Pt/^{195}Pt)|_{ref.sample}]$ (and the same for the other isotopes). Such a description was chosen in order to display overabundances of Pt isotopes of meteorite samples as factors relative to our reference material.

We did not find any significant deviation for ^{196}Pt and ^{194}Pt for AKL, AMW and the ACL samples. The mean values are consistent with its natural values within 2% (0.98–1.00). Individual data for one measurement series, however, show differences of up to 5%. In particular, measurement series Pt_07 seems to be somewhat lower for ^{196}Pt and ^{194}Pt for the nanodiamond samples. Such scatter of the order of 4–5% might be the accuracy of Pt measurements at VERA with slow sequencing (see below). A different picture was found for $^{198}Pt/^{195}Pt$: we see a good agreement for the nanodiamond

Table 2
Measured isotope ratios for reference and nanodiamond samples. The values 0.212, 0.746 and 0.974 are the solar abundance ratios. The uncertainties listed are the standard deviation of the mean values. Larger scatter was observed between different beamtimes indicating rather a total uncertainty in Pt-AMS of 2–3% 2 identical sputter samples were available for reference (^{nat}Pt-1 and ^{nat}Pt-2) and ACL samples (ACL-1 and ACL-2).

Measurement/isotope ratio	$^{198}Pt/^{195}Pt$	$^{196}Pt/^{195}Pt$	$^{194}Pt/^{195}Pt$
Pt_05	*0.212*	*0.746*	*0.974*
^{nat}Pt	0.199 ± 0.003	0.729 ± 0.006	0.945 ± 0.009
^{nat}Pt	0.196 ± 0.002	0.731 ± 0.003	0.963 ± 0.005
ACL	0.206 ± 0.002	0.735 ± 0.005	0.955 ± 0.004
ACL	0.205 ± 0.003	0.735 ± 0.003	0.955 ± 0.005
AKL	–	–	–
AMW	–	–	–
Pt_06	*0.212*	*0.746*	*0.974*
^{nat}Pt	0.203 ± 0.003	0.769 ± 0.006	0.993 ± 0.005
^{nat}Pt	0.206 ± 0.003	0.756 ± 0.004	0.963 ± 0.005
ACL	0.204 ± 0.002	0.750 ± 0.003	0.980 ± 0.004
ACL	0.211 ± 0.002	0.752 ± 0.003	0.981 ± 0.005
AKL	0.218 ± 0.002	0.767 ± 0.005	0.963 ± 0.005
AMW	0.221 ± 0.005	0.773 ± 0.007	0.975 ± 0.008
Pt_07	*0.212*	*0.746*	*0.974*
^{nat}Pt	0.223 ± 0.002	0.796 ± 0.004	0.964 ± 0.005
^{nat}Pt	0.220 ± 0.002	0.793 ± 0.003	0.963 ± 0.004
ACL	0.220 ± 0.001	0.753 ± 0.002	0.962 ± 0.002
ACL	0.219 ± 0.001	0.753 ± 0.002	0.963 ± 0.003
AKL	0.242 ± 0.002	0.782 ± 0.002	0.924 ± 0.003
AMW	0.230 ± 0.002	0.755 ± 0.003	0.966 ± 0.004
Pt_08	*0.212*	*0.746*	*0.974*
^{nat}Pt	0.205 ± 0.002	0.754 ± 0.005	0.997 ± 0.005
^{nat}Pt	–	–	–
ACL	0.208 ± 0.001	0.749 ± 0.002	0.985 ± 0.002
ACL	–	–	–
AKL	0.212 ± 0.002	0.746 ± 0.002	0.981 ± 0.002
AMW	0.228 ± 0.002	0.749 ± 0.002	0.981 ± 0.002

Table 1
Typical detector count rates (Pt events per second) for blank, reference and nanodiamond samples for the various Pt beam times Pt_02 to Pt_08. The detectors were Time-of-Flight in combination with Bragg type ionization chamber (ToF/Bragg), a surface barrier detector (solid state), ToF start signal only (ToF_only), and a compact ionization chamber for energy measurement ($\Delta E/E$).

Pt beam-time	Particle-detector	^{195}Pt rate blank	^{195}Pt rate ^{nat}Pt	^{198}Pt rate $^{198}Pt_{enriched}$	^{195}Pt rate AKL	^{195}Pt rate AMW	^{195}Pt rate ACL
Pt_02	ToF/Bragg	0.3–1	6–18	11–36			
Pt_03	ToF/Bragg	5–20	300–3000	700–4500			
Pt_04	ToF/Bragg	1–10	700–2700	30–630	720	200	600–3100
Pt_05	ToF/Bragg	1–30	1000–2000	1000–3000		30–80	1700–3000
Pt_06	Solid state	5	80–200	100	300–900	100	1500–3500
Pt_07	ToF_only	⩽70	100–370	100–1000	1000–2500	100–700	2500–11000
Pt_08	$\Delta E/E$	12–30	100–400	30–550	5000–7000	500–800	3000–15000

Please cite this article in press as: A. Wallner et al., Stable platinum isotope measurements in presolar nanodiamonds by TEAMS, Nucl. Instr. Meth. B (2012), http://dx.doi.org/10.1016/j.nimb.2012.03.036

Table 3
Pt isotope ratios for the reference sample and the three fractions of nanodiamonds from the Allende meteorite as measured in four beamtimes Pt_05 to Pt_08. Listed are in 3 sections the *nominal* values for $^{198}Pt/^{195}Pt$, $^{196}Pt/^{195}Pt$ and $^{194}Pt/^{195}Pt$, respectively (first line), the *measured* isotope ratio for the reference sample "^{nat}Pt-198" (second line), and the *relative deviation* of measured ratio for the reference sample to the nominal ratios (rel. dev. to $^{198}Pt/^{195}Pt|_{nat}$, third line), i.e. $[(^{198}Pt/^{195}Pt)|_{meas} - (^{198}Pt/^{195}Pt)|_{nat}]/[^{198}Pt/^{195}Pt)|_{nat}]$, and the same for $^{196,194}Pt$. The measured Pt isotope ratios of the three meteorite samples AKL, AMW and ACL are then listed as fractions normalized to the reference material. Only AKL and AMW show significant deviations for $^{198}Pt/^{195}Pt$. No uncertainties are listed because statistical uncertainties and standard deviation during one beamtime were much lower than systematic differences from one beam time to the next (see text).

Sample	Pt_05	Pt_06	Pt_07	Pt_08	Mean	Quantity
$^{198}Pt/^{195}Pt\|_{nat}$	0.212	0.212	0.212	0.212		Natural ratio
^{nat}Pt-198	0.198	0.205	0.222	0.205		$^{198}Pt/^{195}Pt\|_{ref.\ sample}$
rel. dev. to $(^{198}Pt/^{195}Pt)\|_{nat}$	−7%	−3%	+5%	−3%		$[(^{198}Pt/^{195}Pt)\|_{meas} - (^{198}Pt/^{195}Pt)\|_{nat}]/[^{198}Pt/^{195}Pt)\|_{nat}]$
ACL-198	1.04	1.01	0.99	1.01	1.01	$(^{198}Pt/^{195}Pt)\|_{ACL}/(^{198}Pt/^{195}Pt)\|_{natPt-198}$
AKL-198	–	1.07	1.09	1.03	1.06	$(^{198}Pt/^{195}Pt)\|_{AKL}/(^{198}Pt/^{195}Pt)\|_{natPt-198}$
AMW-198	–	1.08	1.04	1.11	1.07	$(^{198}Pt/^{195}Pt)\|_{AMW}/(^{198}Pt/^{195}Pt)\|_{natPt-198}$
$^{196}Pt/^{195}Pt$	0.746	0.746	0.746	0.746		Natural ratio
^{nat}Pt-196	0.730	0.763	0.794	0.754		$^{196}Pt/^{195}Pt\|_{ref.\ sample}$
rel. dev. to $(^{196}Pt/^{195}Pt)\|_{nat}$	−2%	+2%	+6%	+1%		$[(^{196}Pt/^{195}Pt)\|_{meas} - (^{196}Pt/^{195}Pt)\|_{nat}]/[^{196196}Pt/^{195}Pt)\|_{nat}]$
ACL-196	1.01	0.99	0.95	0.99	0.99	$(^{196}Pt/^{195}Pt)\|_{ACL}/(^{196}Pt/^{195}Pt)\|_{natPt-196}$
AKL-196	–	1.01	0.98	0.99	0.99	$(^{196}Pt/^{195}Pt)\|_{AKL}/(^{196}Pt/^{195}Pt)\|_{natPt-196}$
AMW-196	–	1.01	0.95	0.99	0.98	$(^{196}Pt/^{195}Pt)\|_{AMW}/(^{196}Pt/^{195}Pt)\|_{natPt-196}$
$^{194}Pt/^{195}Pt$	0.974	0.974	0.974	0.974		Natural ratio
^{nat}Pt-194	0.954	0.978	0.963	0.997		$^{194}Pt/^{195}Pt\|_{ref.\ sample}$
rel. dev. to $(^{194}Pt/^{195}Pt)\|_{nat}$	−2%	0%	−1%	+2%		$[(^{194}Pt/^{195}Pt)\|_{meas} - (^{194}Pt/^{195}Pt)\|_{nat}]/[^{194}Pt/^{195}Pt)\|_{nat}]$
ACL-194	1.00	1.00	1.00	0.99	1.00	$(^{194}Pt/^{195}Pt)\|_{ACL}/(^{194}Pt/^{195}Pt)\|_{natPt-194}$
AKL-194	–	0.99	0.96	0.98	0.98	$(^{194}Pt/^{195}Pt)\|_{AKL}/(^{194}Pt/^{195}Pt)\|_{natPt-194}$
AMW-194	–	1.00	1.00	0.98	0.99	$(^{194}Pt/^{195}Pt)\|_{AMW}/(^{194194}Pt/^{195}Pt)\|_{natPt-194}$

sample "ACL" with "^{nat}Pt". In contrast, we observe consistently higher values for AKL and AMW compared to the ^{nat}Pt samples [24]. The average for "ACL" fits exactly to the nominal ^{nat}Pt values, but AKL and AMW were measured 6 and 7% higher, respectively. As an example $^{198}Pt/^{195}Pt$ measured isotope ratios for beamtime Pt_07 for the nanodiamond samples are plotted in Fig. 2. The error bars represent statistical uncertainties only, with sample AMW having the lowest and ACL the highest Pt count rates (see also Table 1 and Fig. 1).

5. Discussion

The scatter in the data of the AMS measurements was improved for the last measurement series mainly due to the different detector stations used (Table 1): for the first measurements we utilized the time-of-flight and energy detector. Later we moved continuously up-stream with the detector positions and consequently our data were less vulnerable to small drifts in the setup. The main limitation for more precise data seems to be the switching time between the different masses and a non-linear change in the particle count rate can introduce drifts in the isotopic ratios.

Sample material split into different sample holders and measured in the same beam times can be used to quantify deviations from one sample to another due to different sputtering, cross contaminations, beam transport etc. While for the materials AKL and AMW only a limited amount of material was available, for ^{nat}Pt and ACL we could produce at least 2 sputter cathodes. The differences between such identical samples were between 0% and 3% (see Table 2). The difference of the measured values of reference samples to their nominal values was between 0% and 7% (see

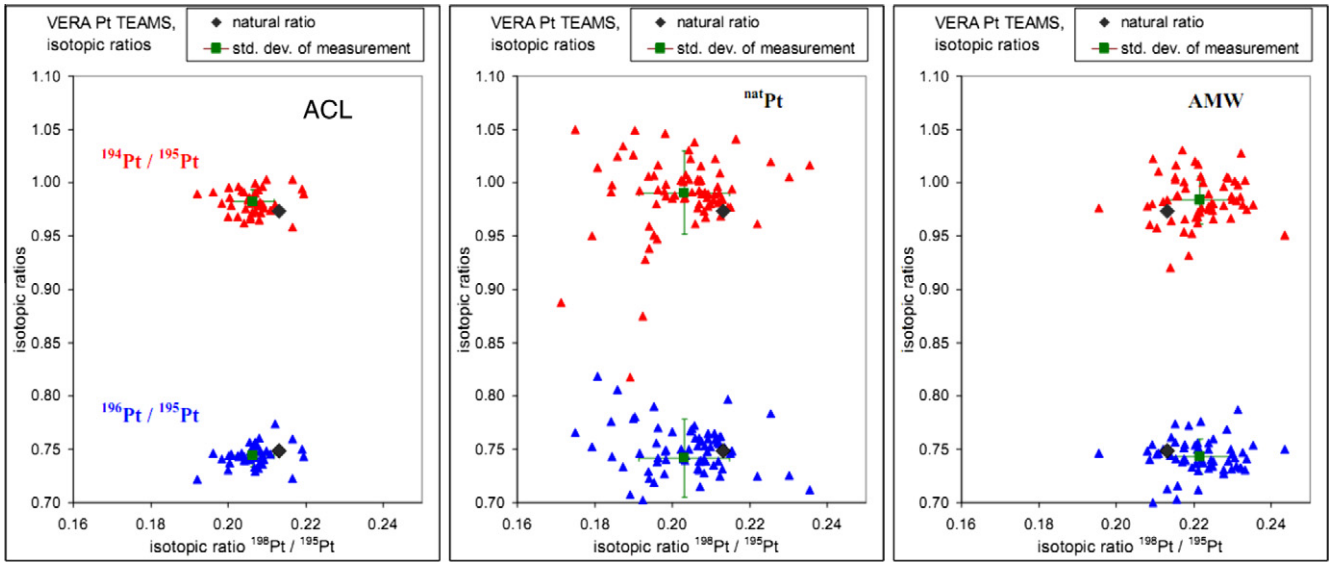

Fig. 1. Example for Pt isotope ratio measurements at VERA. Plotted are individual run results for $^{194}Pt/^{195}Pt$ and $^{196}Pt/^{195}Pt$ versus $^{198}Pt/^{195}Pt$ (triangles). The mean value for a sample is plotted as a green square and its uncertainty represents the standard deviation of one run. For comparison, the natural isotope ratios are indicated by black diamond symbols. ACL (left plot) gives similar values as the ^{nat}Pt samples (2nd plot), although with better counting statistics. The difference of measured to nominal value is believed to be due to different beam transmission for the Pt isotopes. AMW (right plot), however, shows clearly enhanced $^{198}Pt/^{195}Pt$ ratios (data points are shifted to right); while ^{194}Pt and ^{196}Pt correspond to the ^{nat}Pt values. (For interpretation of the references to color in this figure legend, the reader is referred to the web version of this article.)

Please cite this article in press as: A. Wallner et al., Stable platinum isotope measurements in presolar nanodiamonds by TEAMS, Nucl. Instr. Meth. B (2012), http://dx.doi.org/10.1016/j.nimb.2012.03.036

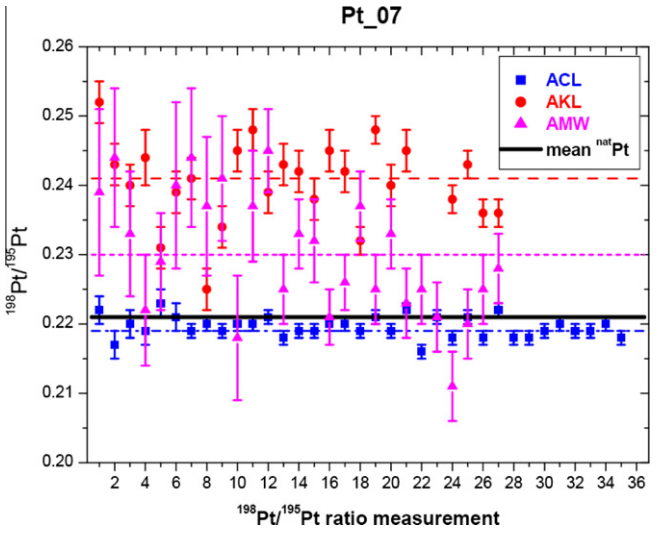

Fig. 2. $^{198}Pt/^{195}Pt$ isotope ratios measured in beamtime Pt_07. Plotted are all ratios for the three nanodiamond samples. The error bars represent statistical uncertainty only. The mean isotope ratio for the three nanodiamonds is shown as dashed lines and for comparison, the black solid line gives the mean $^{198}Pt/^{195}Pt$ ratio obtained for the reference samples. ACL (blue squares) fits well to the reference value while AKL (red circles) and AMW (magenta triangles) are higher in their mean isotope ratio.

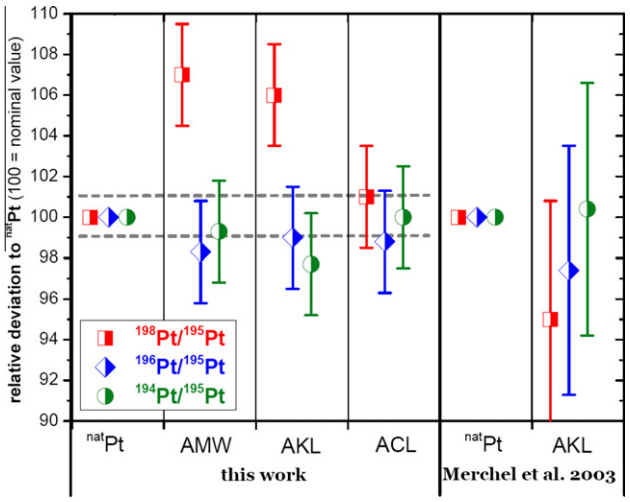

Fig. 3. Isotope ratios for $^{194}Pt/^{195}Pt$ (circles), $^{196}Pt/^{195}Pt$ (diamonds) and $^{198}Pt/^{195}Pt$ (squares) for the reference sample (^{nat}Pt) and the three nanodiamond samples AMW, AKL and ACL. All data are normalized to a value of 100 for ^{nat}Pt. For comparison previous AMS results from [13] are plotted for AKL. The dashed line is an eye-guide only, indicating an uncertainty of ±1%. No error bars were plotted for ^{nat}Pt because all other data were normalized to this value and a minimum uncertainty of ±2% was assumed from systematic contributions. (For interpretation of the references to color in this figure legend, the reader is referred to the web version of this article.)

Table 3). Such differences may originate from slightly different setups for the masses 194, 195, 196 and 198; or may be due to fractionation in the ion source.

To summarize, our averaged data suggest a reproducibility of about 2–3% for Pt measurements at VERA (compared to 5–8% found in [13]). Similar values were found for other heavy ions [25] and also for a series of U and Pu runs for neutron capture cross section measurements of U and Th [26].

The overabundance of ^{198}Pt of 1.06 and 1.07 for AKL and AMW, respectively (see Table 3 and Fig. 3), however, is 2 – 3σ above the expected scatter in the data. All the $^{198}Pt/^{195}Pt$ ratios were consistently above the natural value in all measurements. Such an enhanced $^{198}Pt/^{195}Pt$ isotope ratio is predicted by two models: the neutron burst model [27] and the rapid r-process separation scenario [28]. However, the latter also predicts a strong negative anomaly in $^{194}Pt/^{195}Pt$, which is not observed. The rapid separation predicts almost complete absence of ^{194}Pt. This is because the r-process precursor ^{194}Os has a half-life of ~6 a, so that almost no decay has occurred at the time of the putative separation after ~2 h between r-process precursors and stable end products, a time that has been suggested based on $^{134}Xe/^{136}Xe$ in Xe–H [28,29]. Thus, the Pt results seem to favor the neutron burst model. This is in contrast to the situation in tellurium [15] and adds to the enigma of the nanodiamonds.

6. Summary and outlook

We continued the search for isotopic effects of $^{194,195,196,198}Pt$. As in [13], we used accelerator mass spectrometry, which eliminates molecular interferences, a problem encountered in other mass spectrometric measurements [4].

We observed enhancements in $^{198}Pt/^{195}Pt$ by ~6–7% in two diamond residues from Allende, AKL and AMW, which were prepared by different separation techniques [13]. Data were taken in three different analytical sessions and the effect was reproduced. Variations in other isotopic ratios were within analytical uncertainty of 2–3%, and no anomaly could be identified in a third Allende sample (ACL). An enhanced $^{198}Pt/^{195}Pt$ ratio is predicted by models that either include or exclude a large simultaneous negative anomaly in $^{194}Pt/^{195}Pt$. This negative anomaly, however, was not observed via AMS and is in contrast to data obtained for tellurium.

The reproducibility obtained at VERA on the Pt samples suggests isotope ratios to be precise at levels of 2–3%. However, the robustness of these first results needs to be verified by detailed and systematic studies of possible mass-fractionation effects and potential scatter in the isotope ratios due to a different AMS performance, i.e. differences in sputtering, the beam quality or stability of Pt count rates. These investigations are part of the Eurogenesis programme, a EUROCORES project organized by the European Science foundation [30]. Within this programme Pt measurements will be repeated with sufficient new material extracted from Allende. We plan to extend our measurements in collaboration with ETH Zurich also to other elements.

Acknowledgment

Part of this work was funded by the Austrian Science Fund (FWF): Project No. AP20434 and AI00428 (CoDustMas, Eurogenesis).

References

[1] E. Zinner, Presolar grains, in: H.D. Holland, K.K. Turekian, A. Davis (Eds.), Treatise on Geochemistry Update, Elsevier Ltd, Oxford, p. 1.
[2] R.S. Lewis, G.R. Huss, E. Anders, Y.-G. Liu, R.A. Schmitt, Meteoritics 26 (1991) 363.
[3] I.U. Roederer, J.J. Cowan, A.I. Karakas, K.-L. Kratz, M. Lugaro, J. Simmerer, K. Farouqi, C. Sneden, Astrophys. J. 724 (2010) 975.
[4] Q.-Z. Yin, C.-T.A. Lee, U. Ott, Astrophys. J. 647 (2006) (2006) 676.
[5] G.K. Nicolussi, A.M. Davis, M.J. Pellin, R.S. Lewis, R.N. Clayton, S. Amari, Science 277 (1997) 1281.
[6] M.R. Savina, A.M. Davis, C.E. Tripa, M.J. Pellin, R. Gallino, R.S. Lewis, S. Amari, Science 303 (2004) 649.
[7] E.K. Zinner, F. Moynier, R.M. Stroud, PNAS 2011; published ahead of print April 15, 2011, <http://dx.doi.org/10.1073/pnas.1015118108>.
[8] J.S.A. Krestow, W.E. Kieser, A.E. Litherland, J.C. Rucklidge, G.C. Wilson, X.-L. Zhao, Nucl. Instr. Meth. B259 (2007) 194.
[9] G.C. Wilson, J.C. Rucklidge, L.R. Kilius, G.J. Ding, R.G. Cresswell, Nucl. Instr. Meth. B123 (1997) 583.
[10] S.H. Sie, T.R. Nicklaus, G.F. Suter, Nucl. Instr. Meth. B123 (1997) 558.
[11] R.M. Ender, M. Döbeli, M. Suter, H.A. Synal, Nucl. Instr. Meth. B 123 (1997) 575.
[12] E.J. von Wartburg, PhD ETH Zurich, DISS ETH Nr. 2007; see <http://www.ams.ethz.ch/publications/thesis/vonWartburg.pdf>.

[13] S. Merchel, U. Ott, S. Herrmann, B. Spettel, T. Faestermann, K. Knie, G. Korschinek, G. Rugel, A. Wallner, Geochim. Cosmochim. Acta 67 (2003) 4949.
[14] A. Wallner, Nucl. Instr. Meth. B 268 (2010) 1277.
[15] G.R. Huss, A.P. Koscheev, U. Ott, Meteorit. Planet. Sci. 43 (2008) (2008) 1811.
[16] S. Richter, U. Ott, F. Begemann, Nature 391 (1998) 261.
[17] A. Braatz, U. Ott, T. Henning, C. Jäger, G. Jeschke, Meteorit. Planet. Sci. 35 (2000) 75.
[18] P. Steier, R. Golser, W. Kutschera, A. Priller, C. Vockenhuber, A. Wallner, S. Winkler, Nucl. Instr. Meth. B240 (2005) 445.
[19] P. Steier et al., Nucl. Instr. Meth. B 268 (2010) 1045.
[20] J. Magill, G. Pfennig, J. Galy, Karlsruhe Nuklidkarte, seventh edition, 2006, Revised printing November 2009.
[21] W. Kutschera et al., Nucl. Instr. Meth. B123 (1997) 47.
[22] A. Priller, K. Melber, O. Forstner, R. Golser, W. Kutschera, P. Steier, A. Wallner, Nucl. Instr. Meth. B 268 (2010) 824.
[23] P. Steier, S. Puchegger, R. Golser, W. Kutschera, W. Rom, A. Wallner, E. Wild, Nucl. Instr. Meth. B161–163 (2000) 250.
[24] U. Ott, S. Merchel, K. Melber, A. Wallner, Meteorit. Planet. Sci. 45 (Suppl.) (2010) A159.
[25] P. Steier, E. Hrnecek, A. Priller, F. Quinto, M. Srncik, A. Wallner, G. Wallner, Nucl. Instr. Meth. B (2011). these proceedings.
[26] A. Wallner, T. Belgya, M. Bichler, K. Buczak, I. Dillmann, F. Käppeler, A. Mengoni, F. Quinto, P. Steier, L. Szentmiklosi, J. Korean Phys. Soc. 59 (2011).
[27] B.S. Meyer, D.D. Clayton, L.-S. The, Astrophys. J. 540 (2000) L49.
[28] U. Ott, Astrophys. J. 463 (1996) 344.
[29] Ulrich Ott, Astrid Besmehn, Khalil Farouqi, Oliver Hallmann, Peter Hoppe, Karl-Ludwig Kratz, Karl Melber, Anton Wallner, PASA, 2012, in press, http://dx.doi.org/10.1071/AS11064.
[30] see <http://www.esf.org/activities/eurocores/running-programmes/eurogenesis.html, and http://www.codustmas.eu/>.

Please cite this article in press as: A. Wallner et al., Stable platinum isotope measurements in presolar nanodiamonds by TEAMS, Nucl. Instr. Meth. B (2012), http://dx.doi.org/10.1016/j.nimb.2012.03.036